



Contents lists available at ScienceDirect

Digital Communications and Networks

journal homepage: www.keaipublishing.com/dcan

A geographic routing protocol based on trunk line in VANETs

Chen Chen^{a,b}, Huan Li^{a,*}, Xi'ang Li^b, Jianlong Zhang^{a,c}, Hong Wei^d, Hao Wang^e^a State Key Laboratory of Integrated Services Networks, Xidian University, Xi'an, 710071, China^b Key Laboratory of Industrial Internet of Things & Networked Control, Ministry of Education, Chongqing, 400065, China^c Shanxi Key Laboratory of Integrate and Intelligent Navigation, Xi'an, 710071, China^d China Highway Engineering Consulting Group Co.LTD., Beijing, 101400, China^e Xi'an United Ride Intelligent Technology Co.LTD., Xi'an, 710071, China

ARTICLE INFO

Keywords:

VANETs

AHP

Data transmission routing scheme volume

ABSTRACT

A Trunk Line Based Geographic Routing (TLBGR) protocol in Vehicular Ad-hoc Networks (VANETs) is proposed in this paper to solve the problem of data acquisition in the traditional trunk coordinated control system. Because of the characteristics of short communication time and high packet loss rate among vehicles, the vehicles entering the trunk lines can not transmit their information to the trunk coordinated control system stably. To resolve this problem, the proposed protocol uses the trunk lines' traffic flow and the surrounding road network to provide a real-time data transmission routing scheme. It takes into account the data congestion problem caused by the large traffic flow of the main roads, which leads to the corresponding increase of the information flow of the section and the package loss, and the link partition problem caused by the insufficient traffic flow, which makes the vehicles have to carry and relay information and therefore increase the transmission delay. The proposed TLBGR protocol can be divided into two stages: the next-intersection selection, and the next-hop selection in the chosen path between the current and next intersections. Simulation results show that, compared with other IoT routing protocols including Greedy Perimeter Stateless Routing (GPSR), Ad-hoc On Demand Vector (AODV), and Q-AODV, the TLBGR protocol has better performance in aspects of end-to-end delay, delivery rate, and routing cost under the scenario of urban traffic trunk lines. The TLBGR protocol can effectively avoid data congestion and local optimum problems, increase the delivery rate of data packets, and is therefore suitable for the routing requirements in this application scenario.

1. Introduction

With the rapid development of communication and information technologies [1,2], the Vehicular Ad-hoc Network (VANET) is regarded as a mobile network established for moving vehicles to bridge the gap between the physical and cyber worlds on the wheel [3,4]. It allows vehicles to play the role of nodes and realize the connection among nodes by applying the routing protocol [5,6]. This feature makes the VANET a significant part of the Intelligent Transportation System (ITS) [7,8]. At the same time, with the expanded coverage range of cellular networks, the VANET has great potential in protecting road safety and improving traffic efficiency, although it may bring some new challenges in resource scheduling management [9,10]. After obtaining the information of the vehicle nodes and roads, the VANET could provide road warning, route planning and other services for drivers and passengers [11]. For example,

Xu Z modeled the relationship between truck fuel consumption and driving behavior using data from the Internet of vehicles to design more energy-efficient driving behavior in the soon-to-come era of connected and automated vehicles [12]. Since the dynamics of the network application bring various changes and problems, the routing protocol in the VANET has become an active research field.

Due to the complex topology of urban roads, different application scenarios generate different routing requirements [13]. Traffic trunks run a large amount of traffic in the urban areas. The smooth flow of trunk line plays a decisive role in the traffic conditions of the entire city. Therefore, the trunk coordinated control unit is usually carried out at the intersections. In this way, when most of the traffic flows reach the intersection and the green light signal is working, the vehicles can pass through the intersection without waiting. This is also called green wave control. Among the traditional trunk coordinated control methods, the

* Corresponding author.

E-mail addresses: cc2000@mail.xidian.edu.cn (C. Chen), huanli_Yoly@163.com (H. Li), 155017965@qq.com (X. Li), jlzhang@mail.xidian.edu.cn (J. Zhang), hhwei41@163.com (H. Wei), hhwang41@163.com (H. Wang).<https://doi.org/10.1016/j.dcan.2021.03.001>

Received 27 December 2019; Received in revised form 25 February 2021; Accepted 1 March 2021

Available online xxx

2352-8648/© 2021 Chongqing University of Posts and Telecommunications. Publishing Services by Elsevier B.V. on behalf of KeAi Communications Co. Ltd. This is an

open access article under the CC BY-NC-ND license (<http://creativecommons.org/licenses/by-nc-nd/4.0/>).

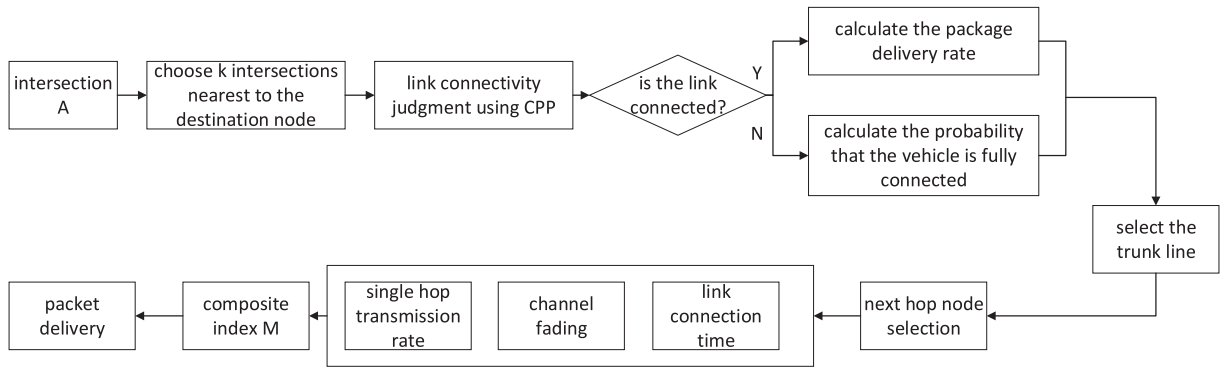


Fig. 1. Overall design framework.

Table 1
Connection Probe Packet (CPP).

Originator: Vehicle ID	ToG: Time stamp	From: Intersection ID	To: Intersection ID
Transmission delay			
Other information			

most classical ones are the graphic method and the numerical method. They are simple and intuitive, but the drawing and calculation processes are relatively complex, easy to cause errors due to human factors. The uneven distribution of traffic in a day also makes it difficult for the trunk coordinated control system to adapt to the changes in traffic volume timely. Besides, the distance between intersections is not uniform, and the speed of vehicles is not controllable, which makes it difficult for the traditional trunk line coordinated control method to achieve real effective green wave control in practical application. In VANETs, the vehicles' real-time driving information can be sent to the trunk coordination control system through the communication networks to solve the above issues, so it is necessary to design an efficient routing protocol for the trunk line network to effectively and fastly transmit vehicular information to the trunk control system.

The routing protocols in VANETs can be divided into four categories: topology based routing protocols, broadcast routing protocols, cluster based routing protocols and location based routing protocols. Ad-hoc On Demand Vector (AODV) [14] is a topology-based routing protocol for Mobile Ad-hoc Network(MANET). When there is a communication demand, the sending node broadcasts the Route Request (RREQ) packet to the neighbor nodes, and the neighbor nodes update the local routing table immediately after receiving it, and then continue to forward the RREQ to their neighbor nodes, and repeat this process until the RREQ is

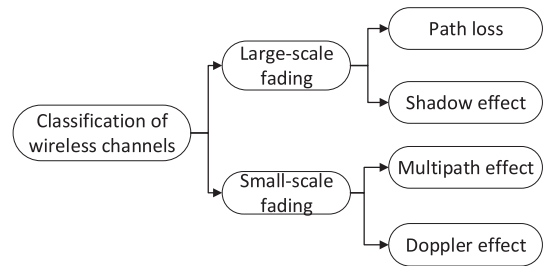


Fig. 4. Wireless channel fading classification.

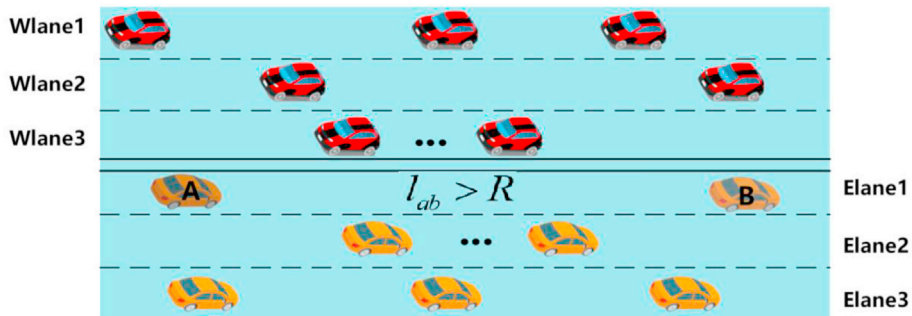


Fig. 2. Overall schematic diagram of network connection.

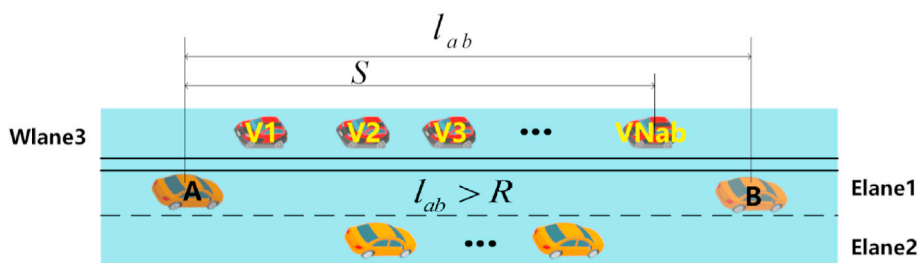


Fig. 3. Local schematic diagram of network connection.

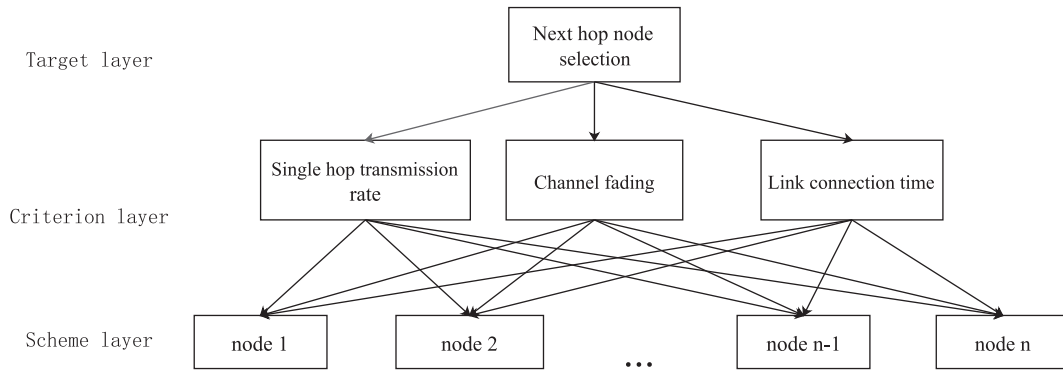


Fig. 5. Hierarchical structure model.

Table 2

Standard values mean random consistency index R.I.

Matrix order	1	2	3	4	5	6	7
RI	0.00	0.00	0.58	0.90	1.12	1.24	1.32

sent to the destination node. However, due to the fast-moving speed of vehicles on the road, the topology of the vehicular network changes quickly, and the communication link quality is low and easy to break. The broadcast routing protocols use the flooding method to send packets to all nodes in the network. The advantage of this kind of routing protocol is that the performance is better when the number of nodes is small, and the destination node can receive messages in a short time, which is suitable for the highway network. But the repeated broadcast of data packet could make the network congested, so it is usually used for vehicles to transmit emergency information. In the cluster-based routing protocol [15], vehicles form vehicle clusters according to their mobility. For each cluster, a cluster head is assigned to communicate with the vehicular nodes inside and outside the cluster. This kind of routing protocol's routing cost is minimal because there is no need to do the routing finding process, and the packet delivery rate is great. However, the protocol does not consider some important parameters such as speed and direction, so the delay is long in a high dynamic network. The Greedy Perimeter Stateless Routing (GPSR) [16] protocol is one of the most classic location-based protocols proposed by Brad Karp. The GPSR protocol uses greedy forwarding and peripheral forwarding in the greedy forwarding failure zone to transmit data packets. It depends on the GPS equipment. Through the GPS, each node knows its location, the locations of its neighbor nodes, and the location of the destination node. Then an optimal path to the target node can be calculated. The node does not need to maintain the routing table or participate in the state information of neighbor nodes. There is no need to establish a global path between the source node and the destination node, so the location-based routing protocol is suitable for the high mobility environment and reduces the network overhead. With the increasing popularity of high-precision maps, 5G communication technologies, and other location services [17,18], the location-based routing protocol has become the primary method. However, it still has some problems in urban scenes, such as excessive hops and routing ring.

In order to improve the performance of the traditional GPSR protocol and provide a real-time data transmission routing scheme which is more suitable for urban trunk information transmission scenarios in VANETs, we propose a new protocol, Trunk Line Based Geographic Routing (TLBGR). The main idea of the TLBGR protocol can be summarized as the following three points:

- Connect Probe Packet (CPP) is used to judge the connectivity of adjacent intersection sections to choose the connected road segment set.

- The optimal road segment is selected under different vehicle densities as the next segment of data packet transmission.
- In the selected optimal section, according to the next hop selection algorithm obtained by the Analytic Hierarchy Process(AHP), the next-hop node is selected.

The rest of the paper is organized as follows. The related work is introduced in Section 2. The geographic routing protocol based on trunk line is introduced in Section 3. Simulation results and analyses are given in Section 4. Section 5 concludes the paper.

2. Related work

2.1. Location-based routing protocol

The GPSR protocol forwards information by one of the broadcast methods: flooding. When multiple broadcast nodes transmit data to the same forwarding node, the number of packets in this node's buffer will increase dramatically [19]. If the packet processing speed is slower than the node's speed of receiving the packet, the transmission delay of the data packet will be greatly increased, and network congestion occurs. In Ref. [20], a privacy-preserving and sparsity-aware location-based prediction method is proposed for collaborative recommender systems. The predictions are made based on both global and spatial nearest neighbors. In 2015, Tianli Hu [21] proposed a node buffer to control network congestion, which improved the performance of the GPSR in the aspect of delay. The scheme determines the routing strategy according to the buffer length and considers not only the distance between the next-hop node and the target node but also the available space of the next-hop node's buffer. This scheme reduces the delay of the route and the packet loss caused by the retransmission waiting time. In 2019, Gao Tianxiang [22] proposed an improved GPSR protocol, in which the road network model and the service quality model are established. The road and intersection location, the effective bandwidth and link lifetime are considered as factors of the service quality model. The forwarding mode does not simply select the closest node to the target node, also executes the segment selection strategy at the intersection and then selects greedy forwarding in the segment. At the same time, the protocol also adopts the carrying and forwarding mechanism to ensure the packet delivery rate in the sparse density environment.

2.2. Trunk-based routing protocol

To design a high-quality information transmission routing protocol on the trunk, there are two key issues: First, how to select the next road segment at the trunk intersection; second, how to select the next-hop vehicle node in the selected segment to propagate the data packet. For the first problem, routing metrics based on specified requirements play a key role in providing quantifiable values to determine the efficiency of protocols. Some routing protocols use the historical traffic information to

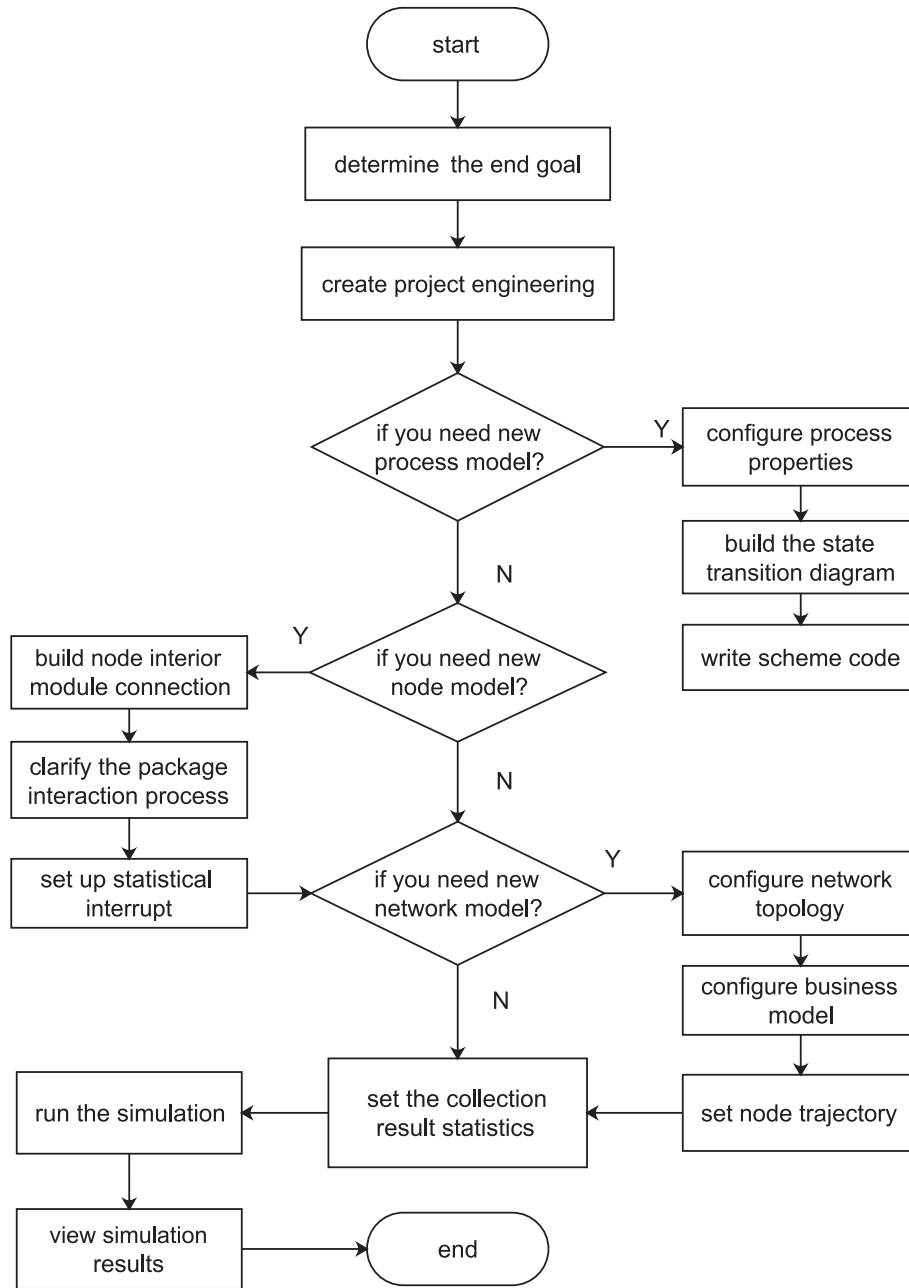


Fig. 6. OPNET simulation process.

design routing metrics such as vehicles' average speed, vehicle density and so on. Vehicles can download the metric data in advance to reduce the communication overhead. The Vehicle Assisted Data Delivery(VADD) [23] method forwards the packets to make sure the lowest transmission delay. The Intersection-based Geographical Routing(IGRP) [24] protocol for VANETs chooses the road segment owning the maximum connectivity based on the quality of service. However, there are two main problems: local maximum capacity and data congestion. Besides, the statistical results of the historical information are not accurate. The VANETs aim to solve the problem of real-time data transmission, but using historical information may lead to sub-optimal routing decisions. For other routing protocols, taking [25] as an example, real-time information is used to calculate the routing metrics. Considering the distribution and movement of nodes, there may be many link partitions, especially in sparse density networks. In this case, it is difficult to calculate the routing metrics. The second question consists of two subparts: how to choose the next-hop vehicle when the packet is transmitted within the road segment,

and how to determine the next-hop vehicle when the packet arrives at the intersection to ensure efficient transmission. The packets cannot always be transmitted according to the pre-computed optimal paths due to the unpredictable topology of the VANET. Therefore, the routing protocol based on trunk lines should apply a method to determine the next segment adaptively to adapt to the changing traffic.

3. Geographic routing protocol based on trunk line

When the traditional GPSR protocol is applied to urban scenes, there are two main problems. On the one hand, when selecting the next link segment, greedily selecting the link nearest to the destination node may lead to a large delay of information transmission due to congestion or low density. On the other hand, the problem of local optimization may exist when the farthest node is selected as the next-hop node in the selected link segment. To solve these problems, the main process of the proposed protocol is shown in Fig. 1. Firstly, some intersections nearest to the

Table 3
OPNET simulation communication parameters settings.

parameter	parameter values
Simulation area size	10000 m*10000 m
Number of lanes	The main road has six lanes in two directions and the other two lanes in two directions.
Number of signal lights	20group
Minimum residence time of vehicles at intersections	3s
Maximum residence time of vehicles at intersections	30s
Minimum vehicle speed	30 km/h
Maximum vehicle speed	60 km/h
Simulation time	3600s
Maximum transmission range of nodes	100 m
Packet size	128bits
Packet type	TIP
Packet generation rate	1-10 packets/s
Beacon size	20bytes
Beacon cycle	2s
Channel capacity	2Mbps
MAC protocol	802.11p

destination node are selected, and the CPP packets are sent to judge the link segment connectivity. Then the link segment with the highest delivery rate is chosen as the next segment. If there is no connecting link, the probability that the vehicle is fully connected in the segment is calculated according to the historical information and the segment with

the highest probability will be chosen. Finally, AHP is used to select the next-hop node for data transmission in the selected link segment considering the single-hop transmission rate, channel fading, and link connection time.

3.1. Hypothesis and system model

Hypothesis: (1) Each vehicle in the VANET can know its position and speed through the GPS and is equipped with a high-precision map to obtain the end position of the road unit through location service. According to the navigation map, each vehicle entering the trunk line equipped with the coordinated control system will trigger the transmission mechanism and send the vehicle traffic information package, which includes the speed of the vehicle, the number of the intersection entering the trunk line, the number of the intersection leaving the trunk line and the number of hops to the pavement system. (2) The urban traffic trunk line is a bidirectional n -lane model ($n \geq 4$). There are pavement units collecting information at both ends of the main traffic lines.

Assuming that each vehicle generates messages at a rate β_s , according to the results in Refs. [15,26], the probability for the vehicle to send a packet in a randomly selected slot is τ_s :

$$\tau_s = \frac{2(1-p)^2}{2 + pW_s - 3p}(T_s\beta_s) \tag{1}$$

Among them, T_s represents the length of a slot and W_s represents the minimum competition window. Suppose there are N vehicles competing

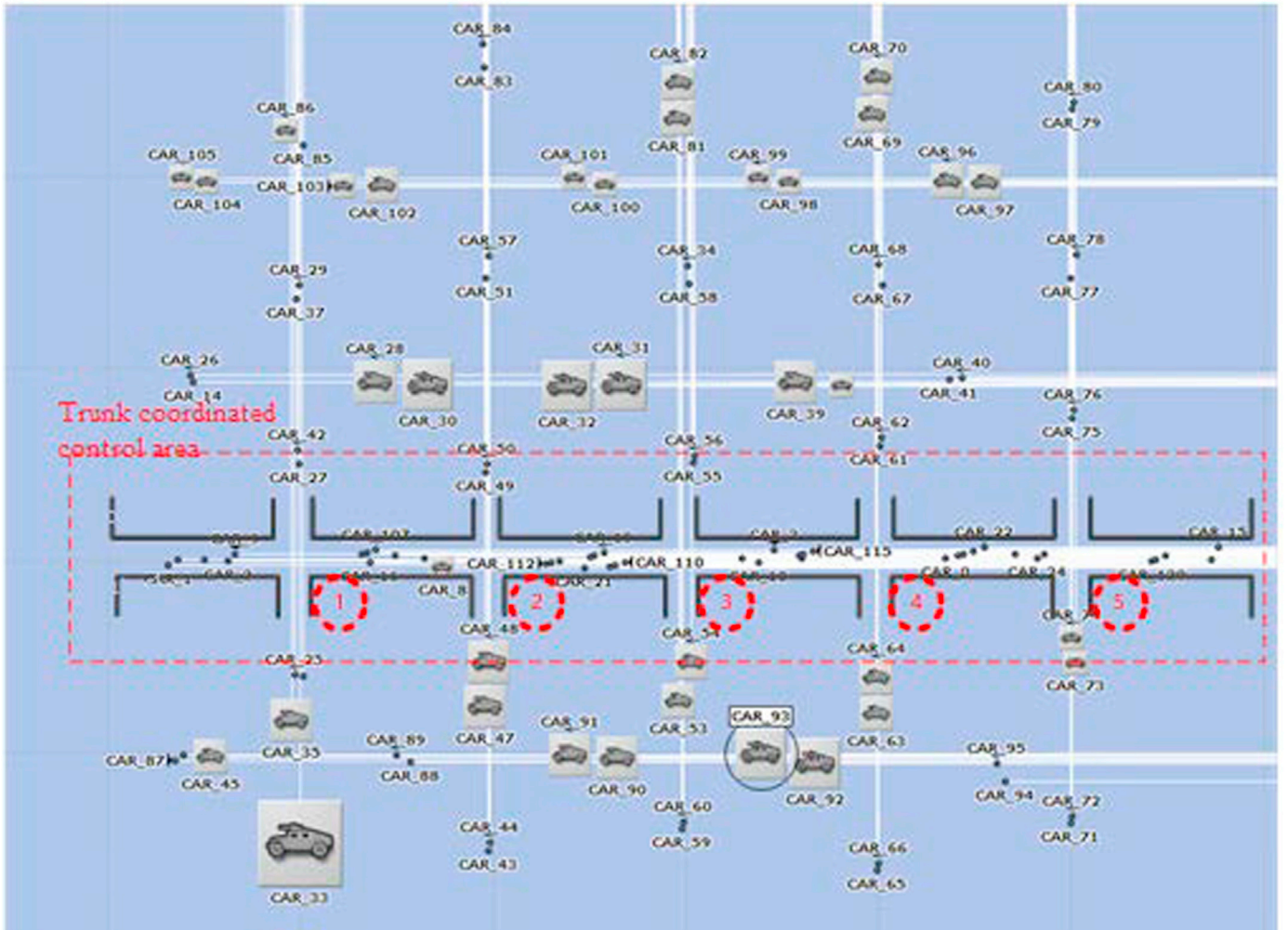


Fig. 7. Simulation network model.

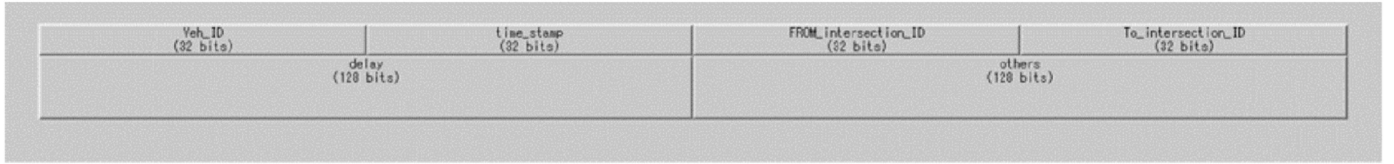


Fig. 8. CPP package in OPNET model.

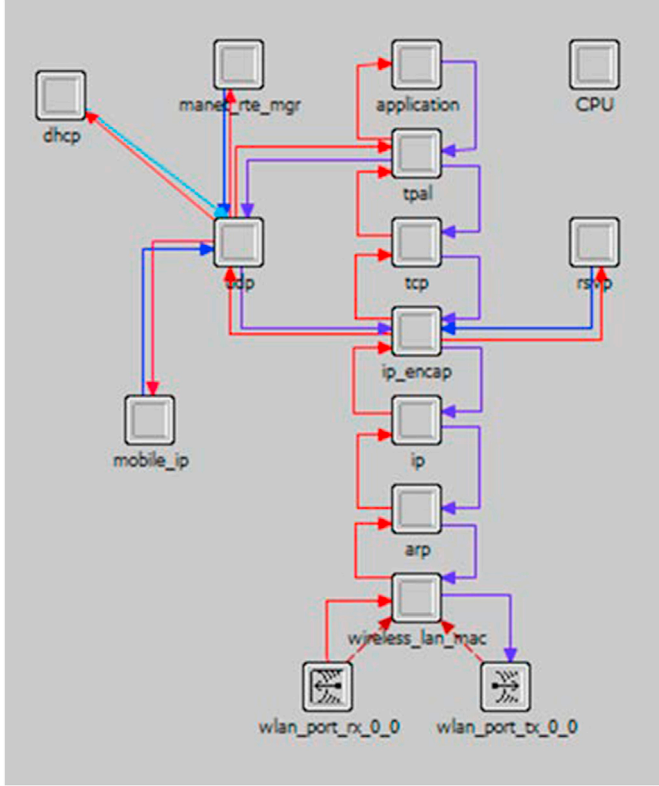


Fig. 9. Node model.

for the same channel with the sending vehicle, then the collision probability of the group access information can be expressed as:

$$p_c = 1 - (1 - \tau_s)^N \quad (2)$$

3.2. Protocol content

In this section, we will use five subsections to introduce the details of the proposed protocol.

3.2.1. Link connectivity decision mechanism for adjacent intersections

The purpose of sending the CPP packets is to detect the link connectivity between two intersections. The format of the CPP package is shown in Table 1. If the result of the adjacent intersection on the traffic trunk is that the link is invalid, the connect probe packet will be sent to the other direction intersections. Time of Generation (ToG) represents the generation time of CPP packets, and other information includes additional routing information such as the average density and the average speed. The connection detection packet is based on the next-hop selection strategy, which transfers hop by hop to traverse the route segment to another intersection. When the connection detection packet arrives at the intersection j , the vehicle nearest to the current intersection v_j is responsible for generating the updated weights. In the connected link segment, it refers to the delivery rate while in the unconnected link segment, it refers to the probability that the vehicle is fully connected.

Then the information is released through the intersection and sent back to the sender v_i . If the CPP does not arrive at the intersection j as planned, the packet will be discarded because of the long delay of this segment. When the connection detection data packet is generated, timer T is triggered. If node v_i receives the data packet from node v_j before timer T fails, the link is determined to be a connection link. Otherwise, it is determined that the segment is invalid.

In summary, the link-connected segments are selected by using the CPP with smaller memory as an alternative route for data packet transmission. And the delivery rate is the primary consideration to select the alternative sections [27] because it is very easy to cause data congestion [28,29] when the urban trunk line carries a large amount of traffic flow [30].

3.2.2. Bidirectional multi-lane multi-hop packet delivery rate modeling

In this section, we will give a flow chart for calculating the delivery rate of bidirectional multi-lane data to solve the problem of data congestion caused by the high density of vehicles on the trunk lines. According to Formula 3, the single-hop transmission rate equals the probability of sending a packet successfully before the specified retry limit r :

$$PDR_{one-hop} = 1 - p_c^r \quad (3)$$

Number of hops: The number of relay nodes that a packet passes through when it is released from one intersection to another via multi-hop transmission.

$d_i, i \in \{1, 2, \dots, n\}$ is defined as every hop process of a sending node in lane i . It is assumed that the average density of vehicles in lane i follows a uniform distribution with parameters λ_i . R represents the transmission radius of a node. The Cumulative Distribution Function (CDF) can be expressed as:

$$P(d_i) = \frac{e^{-\lambda_i(R-d)}(1 - e^{-\lambda_i d})}{1 - e^{-\lambda_i R}} \quad (4)$$

Then, the CDF of the expected multi-lane hopping process is as follows:

$$P(d) = P_1(d)P_2(d)\dots P_n(d) = \frac{e^{-(\lambda_1 + \lambda_2 + \dots + \lambda_n)(R-d)}(1 - e^{-\lambda_1 d})(1 - e^{-\lambda_2 d})\dots(1 - e^{-\lambda_n d})}{(1 - e^{-\lambda_1 R})(1 - e^{-\lambda_2 R})\dots(1 - e^{-\lambda_n R})} \quad (5)$$

Therefore, the expected multi-lane hopping process is as follows:

$$\bar{d} = \int_0^R x dF(x) \quad (6)$$

After knowing the process of each jump in the multi-lane, the expected number of hops can be approximated as follows:

$$h = \frac{L}{\bar{d}} \quad (7)$$

Success rate of multi-hop packet transmission: The overall estimated packet transmission rate of the section can be calculated as follows:

$$PDR_{multi-hop} = (1 - p_c^r)^h \quad (8)$$

When the density of vehicles on the trunk line is low, the data packet

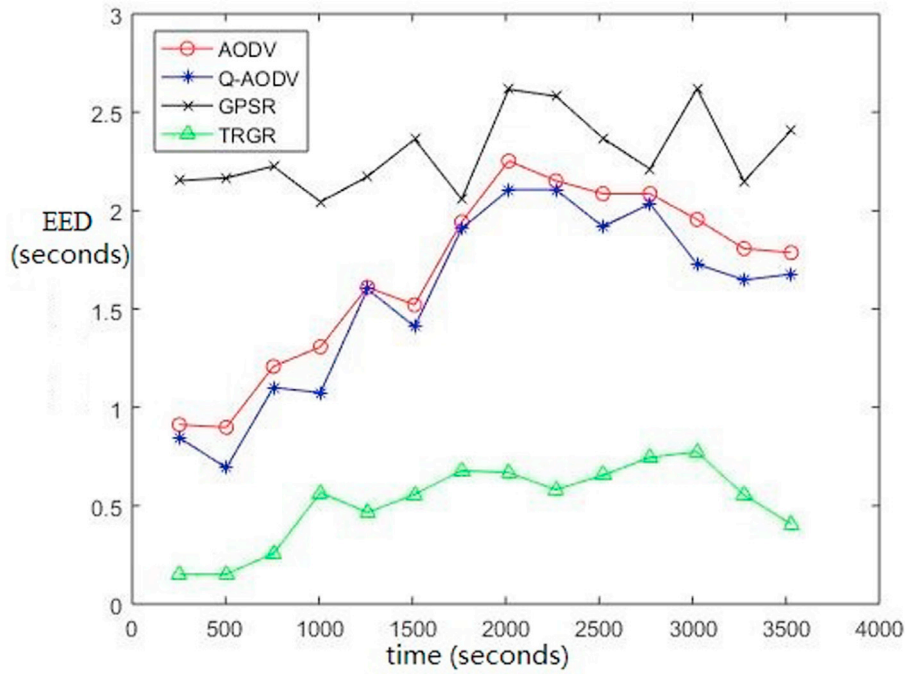


Fig. 10. Transmission delay of four routing protocols.

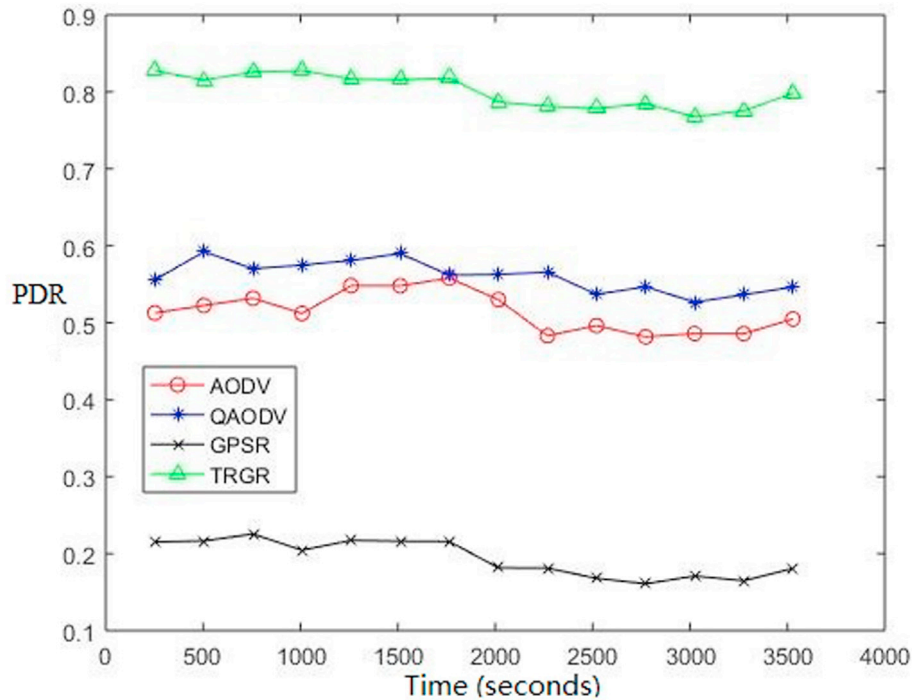


Fig. 11. Delivery rate of four routing protocols.

transmission will encounter the problem of link partition, so only vehicle carrying and forwarding can be selected, which will greatly increase the transmission delay [31]. So in this case, the connection probability of the vehicle network is considered as the primary index.

3.2.3. Complete connection probability modeling

In the transmission phase of CPP, when the link connection is interrupted due to low vehicle density, node v_i can not receive the updated link weight from node v_j . The link weight is estimated by using historical

information through the connectivity of the network, and the link weight becomes the probability that all nodes are connected to each other through wireless communication.

Next, a bidirectional multi-lane network connection analysis model for the urban trunk lines is given. As shown in Fig. 2, for the urban trunk lines, we take the bidirectional six-lane as an example and assume that the average density of vehicles in the lanes obeys the parameters of $\lambda_1, \lambda_2, \dots, \lambda_n$. The uniform distribution of Lane1 is λ_1 , Lane2 is λ_2 and Lane n is λ_n . The number of vehicles on lane i is within interval l , which obeys the

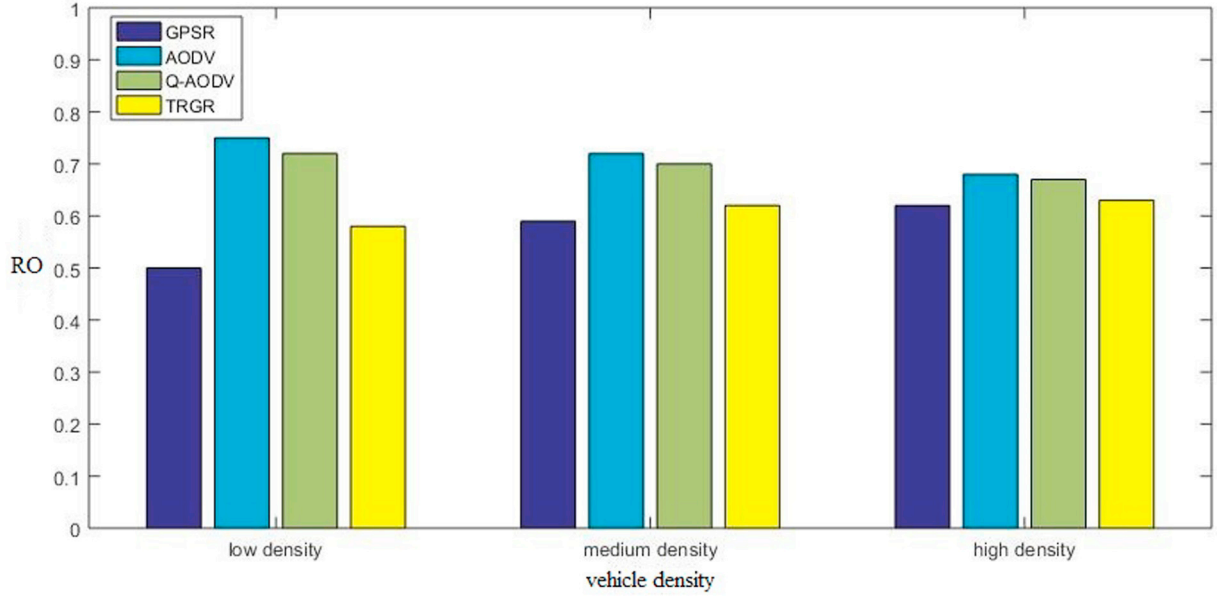


Fig. 12. Comparison of routing overheads under different vehicle densities.

Poisson distribution.

$$f(k_i, l) = \frac{(\lambda_i l)^{k_i}}{k_i!} e^{-\lambda_i l} \quad (9)$$

The distribution function of the workshop distance can be expressed as:

$$F_i(x) = 1 - e^{-\lambda_i x} \quad (10)$$

In the same lane, when the distance between two vehicles running continuously exceeds the transmission distance R of nodes, it is defined as chain breaking. As shown in Fig. 3, the link between vehicle A and vehicle B is disconnected on Lane 4. For the multi-lane link failure, the adjacent lanes can be used to improve the connectivity effect. As shown in Fig. 2, the directional lane on Lane 3 or the adjacent lane on Lane 5 is illustrated in detail with an example of the directional lane, assuming that there are vehicles $V_1 V_2 V_3 \dots V_{N_{ab}}$ in Lane 3 between node A and node B, so vehicles A and B can still be connected by multi-hop relays.

If the following conditions are met, the links between nodes A and B are determined to be connected:

- 1) Condition η_1 : There are at least N_{ab} vehicles in the lane in the gap between vehicles A and B.
- 2) Condition η_2 : In a continuous traffic flow, any workshop distance is shorter than R .
- 3) Condition η_3 : The length of multiple link coverage S is longer than $l_{ab} - R$.

Suppose there is a gap between Lane 3 of the opposite lane including N_{ab_left} vehicles, Lane 5 of the adjacent lane including N_{ab_right} vehicles and Lane 4 of N_{ab} vehicles. If the lane is located on the roadside and there is only one adjacent lane, the probability of one adjacent lane is calculated. According to Formula 5, the probability of the event is:

$$\Pr(\eta_1) = \frac{(\lambda_3 l_{ab})^{N_{ab_left}} e^{-\lambda_3 l_{ab}}}{N_{ab_left}!} + \frac{(\lambda_5 l_{ab})^{N_{ab_right}} e^{-\lambda_5 l_{ab}}}{N_{ab_right}!} + \frac{(\lambda_4 l_{ab})^{N_{ab}} e^{-\lambda_4 l_{ab}}}{N_{ab}!} \quad (11)$$

Medium: $N_{ab_left} \geq N_{ab}, N_{ab_right} \geq N_{ab}$

According to Formula 10, the probability distribution function of the workshop distance less than the maximum transmission distance R of the

vehicle is recorded and defined as $F_i(R) = 1 - e^{-\lambda_i R}$. i represents the number of lanes, so the probability of event η_2 is:

$$F_i(x) = 1 - e^{-\lambda_i x} \quad (12)$$

The probability density function of the corresponding workshop distance is $f_i(x) = \frac{\lambda_i e^{-\lambda_i x}}{1 - e^{-\lambda_i R}}$ and the probability density function of the sum of all vehicle workshop distances can be obtained as follows:

$$f_i(S) = \frac{\lambda_i^m S^{m-1}}{(1 - e^{-\lambda_i R})^m (m-1)!} e^{-\lambda_i S} \quad (13)$$

According to Formula 9, the probability of events can be obtained as follows:

$$\Pr(\eta_3) = 1 - \sum_{i=1}^{i+1} \int_0^{l_{ab}-R} f_i(S) dS \quad (14)$$

Therefore, with the help of multi-hop relay transmission in directional lanes, the probability of events connected by vehicles A and B can be expressed as follows:

$$\Pr(\eta) = \Pr(\eta_1) \Pr(\eta_2) \Pr(\eta_3) \quad (15)$$

According to Ref. [32], the average number of Lane i failure links can be expressed as $N_i = \frac{L}{(e^{\lambda_i R} - 1) \left(\frac{1}{\lambda_i} \frac{R e^{-\lambda_i R}}{1 - e^{-\lambda_i R}} \right) + R + \frac{1}{\lambda_i}}$, so the probability that all

vehicles in Lane 4 will be fully connected by multi-hop transmission is:

$$p_l = [\Pr(\eta)]^{N_i} \quad (16)$$

3.2.4. Next link segment selection

Because of the frequent changes of the topological network and the large scale of the network, it is difficult to get a global understanding of the instantaneous information of the network topology. Therefore, an adaptive intersection selection algorithm is adopted, which can select intersections one by one according to the specified requirements, and calculate the path of each intersection partially continuously. The specific process is as follows:

- 1 Choose the candidate intersections: When a packet arrives at an intersection, there are different candidate intersections defined as adjacent intersections of the current intersections i . In order to reduce

the cost of traversing all intersection to find the best path, we firstly select k suitable candidate intersections in all adjacent intersections collection N_i according to their geographical shortest distance to the destination. This is based on the observed section between the current intersection and its adjacent intersections, so the intersection located on the trunk line is the shortest route to the destination geographically, which often provides the shortest communication path.

2. Choose the best route: In VANET, the connected links should have the priority to be selected in all routes, because the data transmission depends on wireless communication technology and network connection, which will bring lower delay. However, in the presence of multiple links, the path with the greatest connectivity is likely to be the path with the greatest degree of congestion. This may lead to more data collisions, resulting in large latency or low available bandwidth. Therefore, in this case, the transmission rate is considered to be the key parameter reflecting the channel quality. When there are multiple connected routing paths, the aggregation is expressed as $c(i)$. We choose the path with the highest packet transmission rate as the optimal path, that is:

$$l_{optimal} = \operatorname{argmax}_{i \in c(i)} PDR_{multi-hop} \quad (17)$$

Formula 8 is used to calculate the data transmission rate of the routing section. However, for sparse networks, there are likely many link partitions in the network. If the scheme of carry-forward is adopted, the packet will have a higher transmission delay. In this case, connectivity will have significant impact on network performance. Therefore, if all routing paths in set $d(i)$ are disconnected, the path with the greatest connectivity is chosen as the best routing path, that is:

$$l_{optimal} = \operatorname{argmax}_{i \in d(i)} P_i \quad (18)$$

3.2.5. Next hop selection

After the next section is determined, the packet will be forwarded along this section and select the next hop [33,34]. Most routing protocols choose the greedy forwarding mode to select the next hop, which can reduce the number of hops, loss and channel occupancy. However, because the TLBGR protocol is based on the urban traffic trunk lines and the speed of vehicles is relatively fast, the next-hop node selected by greedy forwarding is usually located at the boundary of the transmission range of the sending node. It is likely that the selected vehicle node will drive out of the communication range of the sending node and cause packet loss. Therefore, compared with reducing hops and resource occupancy, the priority should be given to ensuring the reliability of data packet transmission. The time delay can also be eliminated by calculating the formula in the later coordinated control of trunk lines, which has little impact on the entire system.

When choosing an intersection, a selection strategy requiring the next hop to transmit data packets along the selected section. The location of adjacent nodes can be obtained by periodic exchanges of beacon packets. In addition, to ensure the successful transmission of data packets, combined with the communication quality of nodes and the progress of single hop transmission, this protocol uses the AHP to ensure the quality of data packet transmission under trunk demand. Based on the physical characteristics of the urban traffic trunk lines and the application scenarios of this routing protocol, the single hop transmission rate, channel fading and link connection time are selected as the parameters for selecting the next hop. The distance between the vehicles [35] is considered as a factor based on the idea of greedy forwarding. The farther the next hop is from the sending node the closer the destination node, and the smaller the number of hops required, and the corresponding routing overhead will be reduced. However, because the next-hop node farthest from the sending node is always located at the boundary of the transmission range of the node, it is easy to cause packet loss. So we introduce the single hop transmission rate and channel fading as the measurement indexes. This section mainly describes the determination of the distance between

vehicles.

Assuming that there are m potential neighbor nodes in the transmission range of the sending node s , it is defined as a set of all neighbor nodes $N(s) = \{s_1, s_2, s_3, \dots, s_m\}$. The neighbor nodes are filtered by conditions $t_{si} > T_{th}$ to indicate the average link connection time between node s and its neighbor nodes calculated by Formula 21, and then the candidate nodes are identified separately. $L(s, i)$ represents the link connection time between node s and its neighbors, and a threshold value T_{th} is specified for forwarding data packets.

Link connection time refers to the time when direct communication links between two nodes remain continuously available. For the high-speed mobile vehicle network, it is an important basis for judging the quality of communication. The mean and variance of nodes' velocity of node s and node i are defined respectively as $v_s a_s v_i a_i$. $D(t)$ represents the distance between vehicles and the initial value is $D(0) = d_0$. Because of the random mobility of the sum of nodes, the distance between vehicles can be considered as a $G/G/1$ queue, in which the movement of nodes in unit time can be considered as the arrival queue, and the distance between nodes can be considered as the departure queue.

$$p(x|d_0, t) = \Pr(x \leq D(t) \leq x + d_x | d_0) = \frac{1}{\sigma \sqrt{2\pi t}} \sum_{n=-\infty}^{\infty} \left[\exp\left(\frac{\mu x_n^1}{\sigma^2} \frac{[x - d_0 - x_n^1 - \mu t]^2}{2\sigma^2 t}\right) - \exp\left(\frac{\mu x_n''}{\sigma^2} \frac{[x - d_0 - x_n'' - \mu t]^2}{2\sigma^2 t}\right) \right] \quad (19)$$

$$F_{s,i}(t) = 1 - \int_0^R p(x|d_0, t) dx \quad (20)$$

Therefore, the average link connection time can be deduced as:

$$E(T_{s,i}) = \int_0^{+\infty} t dF_{s,i}(t) \quad (21)$$

Channel fading: For a transceiver system from the source node to the destination node, the free space propagation is an ideal wireless signal propagation. It can be understood that the electromagnetic signal emitted by the source node reaches the destination node along a straight line after a certain attenuation. However, for the urban trunk scenario used in this paper, the electromagnetic wave emitted from the source node may reach the destination through a series of reflections. Due to the different phases of arriving at the destination node, the signal strength decreases are different. This process is called channel fading.

As shown in Fig. 4, channel fading is divided into large-scale fading and small-scale fading. Large-scale fading refers to the fading of signals after a long-distance transmission, which can be divided into path loss and shadow effect. Path loss is caused by radiation diffusion of the transmitting power, and the shadow effect is caused by the obstacle blocking signal.

Small-scale fading refers to the instantaneous loss of signals in the transmission process. Small-scale fading can be divided into multipath effect and doppler effect. The multipath effect refers to the interference delay effect caused by the different time of each multipath signal arriving at the receiving node in the multipath transmission, especially in the traffic environment. Doppler frequency shift refers to the phase change caused by the distance difference when the transmitting node moves in a certain direction at a constant rate. When the node moves in front of the wave source, the wavelength becomes shorter, the frequency becomes higher, and the wavelength is compressed [36].

Dedicated Short Range Communications (DSRC) [37] describes that the communication range of a vehicle node in the VANET is usually several hundred meters, so small scale fading is considered. A large number of researchers have confirmed that the nakagami-m channel model has a good fit for the measured experimental data. We define the probability that a packet can be sent from the source node s to the node i after channel fading is C_{si}

$$C_{si} = 1 - \frac{m^m}{\Gamma(m)w^m} \int_0^{t_r} z^{m-1} e^{-\left(\frac{m}{w}\right)z} dz \quad (22)$$

$$t_r = \frac{T_p}{R^2} G \quad (23)$$

$$G = \frac{G_t G_r \lambda}{(4\pi)^2 l} \quad (24)$$

Here, w denotes the average receiving power, t_r is the threshold of the received signal, T_p is the transmitting power, and the G_t , G_r are the antenna gain of the transmitting node and the receiving node, respectively. M denotes the attenuation factor, which represents the severity of channel fading, and is related to the distance between the vehicles required in the previous section. According to the application scenario of the protocol [38], while $50 \leq d(s,i) \leq 150$, m is 1.5. Therefore, the above formula can be simplified as follows:

$$C_{si}(d) = 1 - \frac{1.837d^3}{\Gamma(1.5)} \int_0^{\frac{1}{R^2}} z^{0.5} e^{-1.5z} dz \quad (25)$$

Analytic Hierarchy Process: the AHP is a mathematical tool that can deal with non-quantitative multi-criteria decision-making problems. It is proposed by professor Satie, an American operations researcher, for transforming the complex problems into hierarchical sub-problems to estimate the importance of each metric. In the next hop selection, this method can be used to calculate the weights of the next-hop node and select the next hop node with the largest comprehensive evaluation value [39].

As shown in Fig. 5, the first step is to establish a hierarchical structure model. The target layer, selecting the next node to relay information, is our goal, the second layer is the criterion layer and includes the criteria considered while selecting, and the third layer includes all candidate nodes in which the best one should be chosen to complete the decision.

The second step is to establish the judgment matrix. The weight of each factor is determined by the judgment matrix A . n is the total number of influencing factors in the criterion layer. In this agreement, n takes 3. The judgment matrix has the following properties:

$$a_{ij} = \frac{1}{a_{ji}} \quad (26)$$

$i = 1, 2, 3$ and $j = 1, 2, 3$ represent the three elements' link connection time, single hop transmission rate and channel fading, respectively. 1 represents that element i and element j are equally important, 3 represents that element i is slightly more important than element j , 5 represents that element i is more important than element j , and 7 represents that element i is extremely more important than element j . The established judgment matrix is as follows:

$$A = \begin{pmatrix} 0.0769 & 0.0968 & 0.0476 \\ 0.5385 & 0.6774 & 0.7143 \\ 0.3846 & 0.2258 & 0.2381 \end{pmatrix} \quad (27)$$

Using formula $b_{ij} = \frac{a_{ij}}{\sum_{i=1}^n a_{ij}}$, the normalized matrix is obtained.

$$B = \begin{pmatrix} 0.0769 & 0.0968 & 0.0476 \\ 0.5385 & 0.6774 & 0.7143 \\ 0.3846 & 0.2258 & 0.2381 \end{pmatrix} \quad (28)$$

For each row of normalized matrix B , the eigenvectors obtained by summing the eigenvectors are as follows:

$$w_i = \frac{W_i}{\sum_{i=1}^n W_i} \quad (29)$$

So the weights of link connection time, single hop transmission rate

and channel fading are 0.2213, 1.9302 and 0.8485, respectively. The results show that, compared with link connection time and channel fading, the single hop transmission rate is the most important factor in selecting the next-hop node. Therefore, the composite index is

$$M = 0.0738L(s, i) + 0.6434PDR_{one-hop} + 0.2828C_{si} \quad (30)$$

The third step is matrix consistency test. After normalizing the eigenvector, the sum of all elements in the vector is equal to 1. Matrix consistency means that any element in a matrix satisfies $a_{ij} = a_{ik} a_{kj}$. When the N -order judgment matrix satisfies consistency, its eigenvalues have and only have one value of N . The maximum characteristics of the matrix are computed in Formula 31 and the consistency index is calculated in Formula 32.

Firstly, the maximum characteristics of the matrix are computed.

$$\lambda = \frac{\sum (Aw)_i}{nw_i} \quad (31)$$

Then the Consistency Index (C.I.) is calculated. The consistency index C.I. is the average value of all the remaining eigenvalues in the evaluation judgment matrix after removing the largest eigenvalue in the consistency matrix.

$$C.I. = \frac{\lambda - N}{N - 1} \quad (32)$$

The average Random consistency Index (R.I.) can be obtained by Table 2, and the value of the third-order matrix R.I. is 0.58. Consistency Ratios (C.R.) can be obtained as shown in Formula 33. When C.R. is less than 0.1, the matrix consistency is satisfied. After calculating the above process, the judgment matrix C.R. of this protocol is 0.0356, so the judgment matrix satisfies the consistency test, and the weights set by Formula 29 is reasonable.

$$C.R. = \frac{C.I.}{R.I.} \quad (33)$$

4. Simulation results

4.1. Introduction of simulation tool

OPNET [40,41] is a leading global communication network simulation software, which can simulate wired and wireless networks. It also provides users with a series of simulation models, including various existing network model libraries, communication protocols, node models, etc. On the basis of these simulation models, the users can also modify or build various network models and customize network communication protocols, including the design of network routing, service configuration and node trajectory to realize the simulation of the communication network. In terms of statistical simulation results, the users can build simulation data of probes' corresponding performance indicators, such as Packet Delivery Ratio (PDR) and End-to-End Delay (EED), according to the simulation requirements. OPNET uses C++ programming language and its own core functions to simulate specific communication protocols. The graphical simulation interface also reduces the difficulty of network communication simulation.

Fig. 6 is the basic process of OPNET network simulation. As can be seen from the figure, before using OPNET for simulation, the first step is to see whether there is an available process model according to the function of the user's goal realization. The process model of OPNET is the running position of the simulation source code. If you need to change the source code or create a new source code, you can enter the process model modification/new process as shown in Fig. 6. Then compile and debug until the compilation is passed, the process model is completed. The second step is to check whether a new node model is needed and invoke the process model completed in the previous step with the node model. The model can be built to simulate each layer node of layer 7 according to

Open System Interconnection (OSI) reference model [42,43], or only a new outgoing node and a physical layer antenna can be built according to the simulation needs. The third step is to determine whether a new network layer model is needed and call the node layer model completed in the previous step. According to the simulation requirements, the network topology is set up. Finally, run the simulation and statistical simulation results. At last, the drawing function of MATLAB software is used to import the OPNET software to simulate the data, remove the erroneous data which is obviously deviated, and compare the results.

4.2. Simulation environment and parameter settings

The simulation parameters of OPNET are shown in Table 3. As shown in Fig. 7, the simulation area is 10 km*10 km, the number of vehicles is 100, the main road is two-way 6 lanes, and the other lanes are two-way 2 lanes. The vehicle node trajectory is set by OPNET's Define Trajectory function, and traffic lights are set up at each intersection. In the simulation software, the trajectory and speed of the vehicle are set to simulate the process of slowing down and stopping when the vehicle encounters a red light. The structure model of the CPP is shown in Fig. 8, in which the vehicle ID, time stamp, entry and exit ID account for 32 bits and the delay and other information account for 128 bits. As shown in Fig. 9, the node model is hierarchically designed, which is mainly divided into five layers: the application layer, the transport layer, the network layer, the Media Access Control (MAC) layer and the physical layer.

The application layer is mainly responsible for generating data packets to the lower layer and receiving data packets sent back from the network layer. The transmission layer solves the communication problem from end to end and eliminates the unreliability of the network layer. The network layer is the focus of this research. The TLBGR protocol is designed to organize the neighbor nodes in the network layer to realize the routing function. Different routing protocols can be invoked in the IP node module shown in the figure to achieve the performance comparison of different routing protocols. The MAC layer mainly provides a good interface to the network layer. The PHY layer consists of a set of wireless transceivers to send and receive the bitstreams. In the node model, the function of TPAL module is to adapt to the transport layer and the application layer; the function of IP encap module is to encapsulate the package from the upper layer and transmit it to the lower layer, and to decompose the package from the lower layer and transmit it to the upper layer; the ARP module is the address resolution module which parses the address.

4.3. Simulation index

In order to verify the performance of the TLBGR, the meanings of three indicators are introduced. The application scenario of this protocol is to ensure that the roadside units can obtain real-time traffic data, so the requirement for the data packet delivery rate is very high. Due to the large traffic flow and various communication requirements on the main lines, there are also some requirements for the router cost of this protocol. As a routing protocol for vehicle networking, the delay is also an important evaluation parameter. So we choose three performance indicators: the packet delivery rate, the routing overhead and the end-to-end delay.

- **End-to-End Delay (EED):** The EED refers to the time difference between sending data packets from the source node and receiving data packets from the destination node.
- **Packet Delivery Ratio (PDR):** The PDR is defined as the ratio of the total number of packets received at the destination to the total number of packets generated by the source vehicle.
- **Routing Overheads (RO):** The RO is defined as the ratio between the total byte size of the control packets and the cumulative size of the packets forwarded to the target and the control packets.

4.4. Simulation results and performance analysis

In this section, according to the above simulation settings, the simulation results of different routing protocols obtained by the OPNET simulation software are imported into the MATLAB software. They are compared and analyzed from three aspects: the end-to-end delay, the data packet delivery rate and the routing overhead.

As shown in Fig. 10, the transmission delay of the four routing protocols increases with the increase of traffic flowing into the road network in about 2500 s. The reason is that the more packets are generated in a given period, the more channel the load is, and the additional delay caused by collision and retransmission will increase. For the GPSR protocol, without considering the vehicle traffic, the data packet may encounter maximum local or data congestion, which results in poor performance in terms of delay. Compared with the other three protocols, the TLBGR has the best performance because it adopts an adaptive intersection selection scheme which determines the intersection one by one according to the link weights. For the TLBGR, when choosing the next section, the connection section with the highest package delivery rate is preferred. In addition, if there are no connected sections, the section with the greatest connectivity is selected as the next section to forward data packets. The protocol minimizes the use of a carry-forward strategy and therefore reduces the transmission delay.

Fig. 11 shows the packet delivery rates of the four routing protocols as the simulation proceeds. In the VANET, due to the mobility and density of nodes, there may be some link partitions in the network. Then, the packets sent should be stored and carried until the next hop is found. Due to the size limitation of the buffer, upcoming new packages may be deleted when the buffer is full. Therefore, when the number of vehicles entering the road network increases near 2500 s, the data packet delivery rate of the four routing protocols decreases, especially the GPSR protocol. For the GPSR, because of the occlusion of wireless signals by buildings in cities, greedy forwarding is limited. In the case of optimum local problems, the construction of planar maps will lead to network partition of vehicular networks, and many data packets may be lost, so the performance of the data packet delivery rate implemented by the GPSR is the worst. Because each node of the topology-based protocol maintains the routing table, although the cost of routing establishment and maintenance is relatively high, it guarantees a relatively good data packet delivery rate. So the AODV protocol is better than the GPSR protocol in terms of delivery rate. The TLBGR protocol is based on guaranteeing the data packet delivery rate in section selection and next-hop selection. According to the collected connectivity and delivery rate, appropriate weights are allocated for each road, and then relay nodes are determined one by one. This protocol can greatly reduce data packet loss.

According to Fig. 12, the effects of different vehicle densities on the routing overhead of the four routing protocols are shown. In the topology-based routing protocol, each node has to maintain a routing table containing the information of each node in the network continuously. The continuous routing establishment and maintenance process result in high overhead. Therefore, the routing overheads of the AODV protocol and the Q-AODV protocol are higher than that of the GPSR protocol under different vehicle density conditions. For the GPSR protocol and the TLBGR protocol, vehicles can obtain their own location information through the vehicle-mounted GPS and exchanging information with other vehicles. The source node places the location information of the destination node into the header of the packet without establishing and maintaining the update routing table, so the routing overhead is relatively low. For the GPSR protocol, the increase of the number of nodes leads to the increase of routing overhead because the rate of the control packet is proportional to the number of nodes. For the TLBGR protocol, regardless of the vehicle density, it is necessary to evaluate the link weight and assign an appropriate weight to each link, which also leads to a considerable routing overhead. In fact, the reservation and allocation of the resources in Mobile Cloud Computing (MCC) can reduce the routing overhead and improve the computing speed [44,

45].

5. Summary

According to the actual demand for coordinated control of urban trunk lines, this paper creatively proposes the TLBGR protocol. Routing forwarding is carried out according to the sequence of the next hop after choosing the section first. Under the condition of the high-density network, we use the index of data packet delivery rate as the criterion for road section selection, and propose a method for calculating the data packet delivery rate in the two-way multi-lane road network. In sparse networks, the next segment with higher link connectivity will be selected first. There are many factors to be considered when choosing the next hop. According to the single hop transmission rate, channel fading and single hop transmission rate as evaluation indicators, the next hop selection of neighbor nodes is judged using the analytic hierarchy process. Finally, the simulation software OPNET is used to evaluate the end-to-end delay, the data packet delivery rate and the routing overhead of the TLBGR protocol. The results show that the TLBGR protocol performs better than the other three protocols, namely, GPSR, AODV and Q-ARDV, in the urban trunk network environment. In the future, we will take into account the mobile devices held by pedestrians for information exchange, and attempt to address the information security and privacy issues in trajectories sharing and prediction [27,46], edge-cloud cooperation [31,47,48], private data transmission [49,50], etc. In addition, we will optimize the weight determination method by machine learning [51] and try to consider the trunk coordination control algorithm based on the collected video and audio [52,53] information using the TLBGR.

Declaration of competing interest

We declare that we do not have any commercial or associative interest that represents a conflict of interest in connection with the work submitted.

Acknowledgements

This work was supported by the National Key Research and Development Program of China (2017YFE0121400), the National Natural Science Foundation of China (61571338, U1709218, 61672131), the Key Program of NSFC-Tongyong Union Foundation (U1636209), the key research and development plan of Shaanxi province (2017ZDCXL-GY-05-01, 2019ZDLGY13-04, 2019ZDLGY13-07), the Xi'an Key Laboratory of Mobile Edge Computing and Security (201805052-ZD3CG36) and the 111 Project of China (B08038) and the Innovation Fund of Xidian University (5001-20109195456).

References

- [1] T. Yang, Z. Jiang, R. Sun, N. Cheng, H. Feng, Maritime search and rescue based on group mobile computing for uavs and usvs, *IEEE Transactions on Industrial Informatics* (2020), <https://doi.org/10.1109/TII.2020.2974047>.
- [2] Jie Feng, F Richard Yu, Qingqi Pei, Xiaoli Chu, Jianbo Du, Li Zhu, Cooperative computation offloading and resource allocation for blockchain-enabled mobile edge computing: a deep reinforcement learning approach, *IEEE Internet of Things J* 7 (7) (2020) 6214–6228.
- [3] Huansheng Ning, Hong Liu, Jianhua Ma, Laurence T. Yang, and Runhe Huang Cybermatics: Cyber-physical-social-thinking hyperspace based science and technology. *Future Generat. Comput. Syst.*, page S0167739X15002356.
- [4] Huansheng Ning, Hong Liu, Cyber-physical-social based security architecture for future internet of things, *Adv. Internet Things* 2 (1) (2012) 1.
- [5] Chen Chen, Hongyu Xiang, Tie Qiu, Cong Wang, Yang Zhou, Victor Chang, A rear-end collision prediction scheme based on deep learning in the internet of vehicles, *J. Parallel Distr. Comput.* 117 (2018) 192–204.
- [6] Chen Chen, Qingqi Pei, Xiaojie Li, A gts allocation scheme to improve multiple-access performance in vehicular sensor networks, *IEEE Trans. Veh. Technol.* 65 (3) (2015) 1549–1563.
- [7] Yun Yang, Donghai Li, Zongtao Duan, Chinese vehicle license plate recognition using kernel-based extreme learning machine with deep convolutional features, *IET Intell. Transp. Syst.* 12 (3) (2017) 213–219.
- [8] X. Li, J. Li, Y. Liu, Z. Ding, A. Nallanathan, Residual transceiver hardware impairments on cooperative noma networks, *IEEE Trans. Wireless Commun.* 19 (1) (2020) 680–695.
- [9] Y. Li, H. Celebi, M. Daneshmand, C. Wang, Energy-efficient femtocell networks: challenges and opportunities, *Wireless Communications IEEE* 20 (6) (2013) 99–105.
- [10] Yun Li, Chao Liao, Yong Wang, Chonggang Wang, Energy-efficient optimal relay selection in cooperative cellular networks based on double auction, *IEEE Trans. Wireless Commun.* 14 (8) (2015) 4093–4104.
- [11] Chen Chen, Cong Wang, Tie Qiu, Mohammed Atiqzaman, Dapeng Oliver Wu, Caching in vehicular named data networking: architecture, schemes and future directions, *IEEE Commun. Surv. Tutor.* (2020).
- [12] Zhigang Xu, Wei Tao, Said Easa, Xiangmo Zhao, Xiaobo Qu, Modeling relationship between truck fuel consumption and driving behavior using data from internet of vehicles, *Comput. Aided Civ. Infrastruct. Eng.* 33 (3) (2018) 209–219.
- [13] Manuel Schiller, Marius Dupius, Daniel Krajzewicz, Andreas Kern, Alois Knoll, Multi-resolution traffic simulation for large-scale high-fidelity evaluation of vanet applications, in: *Simulating Urban Traffic Scenarios*, Springer, 2019, pp. 17–36.
- [14] Satish Anamalamudi, Abdur Rashid Sangi, Mohammed Alkathiri, Ahmedin Mohammed Ahmed, Aodv routing protocol for cognitive radio access based internet of things (iot), *Future Generat. Comput. Syst.* 83 (2018) 228–238.
- [15] Lei Liu, Chen Chen, Tie Qiu, Mengyuan Zhang, Siyu Li, Bin Zhou, A data dissemination scheme based on clustering and probabilistic broadcasting in vanets, *Vehicular Communications* 13 (2018) 78–88.
- [16] Adam Walker, Milena Radenkovic, Gpsr-tars: congestion aware geographically targeted remote surveillance for vanets, in: *2017 International Conference on Selected Topics in Mobile and Wireless Networking (MoWNeT)*, IEEE, 2017, pp. 1–6.
- [17] Rui Lai, Yang Yin-tang, Total variation regularized back-projection method for spatial resolution enhancement, *IEEJ Trans. Electr. Electron. Eng.* 10 (2015). S55–S59.
- [18] Li Song, Qiang Ni, Yanjing Sun, Geyong Min, Saba Al-Rubaye, Energy-efficient resource allocation for industrial cyber-physical iot systems in 5g era, *IEEE Transactions on Industrial Informatics* 14 (6) (2018) 2618–2628.
- [19] Yanjing Sun, Bowen Wang, Li Song, Zhi Sun, Hien M. Nguyen, Trung Q. Duong, Manipulation with domino effect for cache-and buffer-enabled social iot: preserving stability in tripartite graphs, *IEEE Transactions on Industrial Informatics* (2019).
- [20] Shunmei Meng, Lianyong Qi, Qianmu Li, Wenmin Lin, Xiaolong Xu, Shaohua Wan, Privacy-preserving and sparsity-aware location-based prediction method for collaborative recommender systems, *Future Generat. Comput. Syst.* 96 (2019) 324–335.
- [21] Tianli Hu, Minghui Liwang, Lianfen Huang, Yuliang Tang, An enhanced gpsr routing protocol based on the buffer length of nodes for the congestion problem in vanets, in: *2015 10th International Conference on Computer Science & Education (ICCSE)*, IEEE, 2015, pp. 416–419.
- [22] Tianxiang Gao, Ying Shi, Ziwei Liu, Longchang Wu, School of Automation, Gpsr improvement protocol based on road network and qos model, *Computer Engineering*, 2019.
- [23] Jing Zhao, Guohong Cao, Vadd: vehicle-assisted data delivery in vehicular ad hoc networks, *IEEE Trans. Veh. Technol.* 57 (3) (2008) 1910–1922.
- [24] Hanan Saleet, Rami Langar, Kshirasagar Naik, Raouf Boutaba, Amiya Nayak, Nishith Goel, Intersection-based geographical routing protocol for vanets: a proposal and analysis, *IEEE Trans. Veh. Technol.* 60 (9) (2011) 4560–4574.
- [25] Jacek Rak Lla, A new anypath routing scheme providing long path lifetime in vanets, *IEEE Commun. Lett.* 18 (2) (2013) 281–284.
- [26] Khalid Abdel Hafeez, Lian Zhao, Bobby Ma, Jon W. Mark, Performance analysis and enhancement of the dsrc for vanet's safety applications, *IEEE Trans. Veh. Technol.* 62 (7) (2013) 3069–3083.
- [27] Ou Lu, Qin Zheng, Shaolin Liao, Hong Yuan, Xiaohua Jia, Releasing correlated trajectories: towards high utility and optimal differential privacy, *IEEE Trans. Dependable Secure Comput.* (2018).
- [28] Chen Chen, Tie Qiu, Jinna Hu, Zhiyuan Ren, Yang Zhou, Arun Kumar Sangaiah, A congestion avoidance game for information exchange on intersections in heterogeneous vehicular networks, *J. Netw. Comput. Appl.* 85 (2017) 116–126.
- [29] Runmin Wang, Zhigang Xu, Xiangmo Zhao, Jinchao Hu, V2v-based method for the detection of road traffic congestion, *IET Intell. Transp. Syst.* 13 (5) (2019) 880–885.
- [30] Zongtao Duan, Yun Yang, Kai Zhang, Yuanyuan Ni, Saurab Bajgain, Improved deep hybrid networks for urban traffic flow prediction using trajectory data, *IEEE Access* 6 (2018) 31820–31827.
- [31] Bowen Wang, Yanjing Sun, Li Song, Cao Qi, Hierarchical matching with peer effect for low-latency and high-reliable caching in social iot, *IEEE Internet of Things Journal* 6 (1) (2018) 1193–1209.
- [32] Andre B. Reis, Susana Sargento, Filipe Neves, Ozan K. Tonguz, Deploying roadside units in sparse vehicular networks: what really works and what does not, *IEEE Trans. Veh. Technol.* 63 (6) (2013) 2794–2806.
- [33] Bowen Wang, Yanjing Sun, Zhichao Sheng, Hien M. Nguyen, Trung Q. Duong, Inconspicuous manipulation for social-aware relay selection in flying internet of things, *IEEE Wireless Communications Letters* (2019).
- [34] Bowen Wang, Yanjing Sun, Hien M. Nguyen, Trung Q. Duong, A novel socially stable matching model for secure relay selection in d2d communications, *IEEE Wireless Communications Letters* (2019).
- [35] Chen Chen, Xiaomin Liu, Tie Qiu, Lei Liu, Arun Kumar Sangaiah, Latency estimation based on traffic density for video streaming in the internet of vehicles, *Comput. Commun.* 111 (2017) 176–186.

- [36] D. Dong, M. Wang, W. Chen, Z. Zeng, L. Song, Q. Zhang, M. Cai, Y. Cheng, J. Lv, Mitigation of multipath effect in gnss short baseline positioning by the multipath hemispherical map, *J. Geodes.* 90 (3) (2016) 255–262.
- [37] Zhigang Xu, Xiaochi Li, Xiangmo Zhao, Michael H. Zhang, Zhongren Wang, Dsrc versus 4g-lte for connected vehicle applications: a study on field experiments of vehicular communication performance, *J. Adv. Transport.* 2017 (2017).
- [38] Xiaomin Ma, Xiaoyan Yin, M. Wilson, K.S. Trivedi, Mac and application-level broadcast reliability in vanets with channel fading, in: *International Conference on Computing*, 2013.
- [39] Mehdi Asghari, Parvin Nassiri, Mohammad Reza Monazzam, Farideh Golbabaie, Hossein Arabalibeik, Aliakbar Shamsipour, Armin Allahverdy, Weighting criteria and prioritizing of heat stress indices in surface mining using a delphi technique and fuzzy ahp-topsis method, *Journal of Environmental Health Science and Engineering* 15 (1) (2017) 1.
- [40] Yu Zhang, Yong Zhang, Xiaozhuo Li, Chuqiao Wang, Haihao Li, Simulation platform of leo satellite communication system based on opnet, in: *Fourth Seminar on Novel Optoelectronic Detection Technology and Application*, vol. 10697, International Society for Optics and Photonics, 2018, 106975C.
- [41] Maryam Pahlevan, Roman Obermaisser, Evaluation of time-triggered traffic in time-sensitive networks using the opnet simulation framework, in: *2018 26th Euromicro International Conference on Parallel, Distributed and Network-Based Processing (PDP)*, IEEE, 2018, pp. 283–287.
- [42] Zhenning Wang, Jun Yang, Rami Melhem, Bruce Childers, Youtao Zhang, Minyi Guo, Quality of service support for fine-grained sharing on gpus, in: *ACM SIGARCH Computer Architecture News*, vol. 45, ACM, 2017, pp. 269–281.
- [43] John D. Day, Hubert Zimmermann, The osi reference model, *Proc. IEEE* 71 (12) (1983) 1334–1340.
- [44] Yun Li, Jie Liu, Bin Cao, Chonggang Wang, Joint optimization of radio and virtual machine resources with uncertain user demands in mobile cloud computing, *IEEE Trans. Multimed.* (9) (2018), 1–1.
- [45] Lei Liu, Chen Chen, Qingqi Pei, Sabita Maharjan, and Yan Zhang. Vehicular Edge Computing and Networking: A Survey. *Mobile Networks and Applications*, pages 1–24.
- [46] Rui Zhang, Peng Xie, Chen Wang, Gaoyang Liu, Shaohua Wan, Classifying transportation mode and speed from trajectory data via deep multi-scale learning, *Comput. Network.* 162 (2019) 106861.
- [47] Yupeng Hu, Yonghe Liu, Wenjia Li, Keqin Li, Kenli Li, Nong Xiao, Qin Zheng, Unequal failure protection coding technique for distributed cloud storage systems, *IEEE Transactions on Cloud Computing* (2017).
- [48] Jixin Zhang, Kehuan Zhang, Qin Zheng, Hui Yin, Qixin Wu, Sensitive system calls based packed malware variants detection using principal component initialized multilayers neural networks, *Cybersecurity* 1 (1) (2018) 10.
- [49] Boyang Wang, Baochun Li, Hui Li, Panda: public auditing for shared data with efficient user revocation in the cloud, *IEEE Transactions on services computing* 8 (1) (2013) 92–106.
- [50] Boyang Wang, Xinxin Fan, Search ranges efficiently and compatibly as keywords over encrypted data, *IEEE Trans. Dependable Secure Comput.* 15 (6) (2016) 1027–1040.
- [51] Linbo Wang, Zhen Hui, Xianyong Fang, Shaohua Wan, Weiping Ding, Yanwen Guo, A unified two-parallel-branch deep neural network for joint gland contour and segmentation learning, *Future Generat. Comput. Syst.* 100 (2019) 316–324.
- [52] Songtao Ding, Shiru Qu, Yuling Xi, Shaohua Wan, Stimulus-driven and concept-driven analysis for image caption generation, *Neurocomputing* (2019).
- [53] Rui Lai, Juntao Guan, Yintang Yang, Ai Xiong, Spatiotemporal adaptive nonuniformity correction based on btv regularization, *IEEE Access* 7 (2018) 753–762.